NIH Public Access
Author Manuscript
Acc Chem Res. Author manuscript; available in PMC 2014 November 19.

Published in final edited form as:
Acc Chem Res. 2013 November 19; 46(11): . doi:10.1021/ar400010v.

Biomedical and Biochemical Applications of Self-Assembled Metallacycles and Metallacages

Timothy R. Cook[†], **Vaishali Vajpayee**[‡], **Min Hyung Lee**[‡], **Peter J. Stang**[†], and **Ki-Whan Chi**[‡]
[†]Department of Chemistry, University of Utah, 315 South 1400 East, Salt Lake City, Utah, U.S.A
[‡]Department of Chemistry, University of Ulsan, Ulsan 680-749, Republic of Korea

Conspectus

Coordination-driven self-assembly utilizes the spontaneous formation of metal-ligand bonds in solution to drive mixtures of molecular building blocks to single, unique 2D metallacycles or 3D metallacages based on the directionality of the precursors used. The supramolecular coordination complexes (SCCs) obtained via this process are characterized by well-defined internal cavities and facile pre- or post-self-assembly functionalizations. These properties augment the modularity of the directional bonding design strategy to afford structures with unprecedented tunability both spatially and electronically. Over the past decades, a number of synthetic design methodologies have become established which has led to a substantial library of complexes supported by numerous structural studies. More recently, there has been an emergence of research centered on the potential applications of SCCs, which has developed rapidly on the foundations provided by the aforementioned synthetic and structural bodies of work.

The necessary presence of metal ions as structural elements for the directional bonding approach can be exploited to provide biological activity to an SCC, particularly for Pt and Ru-based structures. Since these two metals are not only among the most commonly used for coordination-driven self-assembly but are also the basis for a number of small molecule anticancer agents, a growing number of SCCs have been evaluated for their antitumor properties. When the internal cavity of a cage is optimized for guest encapsulation, a second vector for biological activity, namely drug delivery, is unlocked. Since cages can offer both inherent activity due to their metal ions, as well as delivery of exogenous drug molecules, such ensembles are particularly promising chemotherapeutic agents.

The non-covalent interactions of SCCs with guest molecules oftentimes manifest photophysical changes to the resulting host/guest complex. Since a metallacage or cycle can be readily tuned to match a specific guest, certain SCCs are well-suited to act as fluorescence-based sensors for biologically relevant analytes. These interactions are not limited to small molecule analytes, however, and SCCs are increasingly being studied for their chemistry with macro biomolecules including DNA and proteins. In particular, dinuclear iron and ruthenium-based helicates bind to a variety of DNA constructs through non-covalent mechanisms. Studies concerning these cylindrical SCCs, which have expanded beyond Ru and Fe, often include characterizations of specific interactions with DNA or other biomolecules. Such investigations are not limited to dinuclear M_2L_3 helicates; Pt-based squares are well-suited to stabilize G-quadruplex DNA and rhomboid metallacycles can unravel supercoiled DNA, further demonstrating the versatility of multinuclear supramolecular architectures. Understanding these interactions in the context of observed cytotoxicities and other biological consequences is critical for developing new chemotherapeutic agents and developing mechanistic models for any biological activity observed using in vitro and in vivo assays.

Correspondence to: Timothy R. Cook; Peter J. Stang.

NIH-PA Author Manuscript
NIH-PA Author Manuscript
NIH-PA Author Manuscript

NIH-PA Author Manuscript

NIH-PA Author Manuscript

NIH-PA Author Manuscript

Introduction

The use of synthetic coordination complexes in biological settings is a logical extension of the studies of natural systems which reveal that, despite a common association of biochemistry with organic molecules and transformations, metal ions and complexes are found ubiquitously. The compatibility of metal ions with biology is forecasted by the variety of Lewis-basic sites found on biomolecules, ranging from the hydroxyl groups of sugars, the carboxylate, amine, and certain side-chain groups of amino acids, the *N*-heterocyclic rings of nucleotides and nucleic acids and other heterocycles, such as porphyrin rings, to name a few.[1] Bulk metal ions of Na, K, Mg and Ca constitute as much as one percent of human body weight.[2] The remaining trace ions, most commonly of Fe, Ni, Cu, Mn, Zn, Co, Mo and V, make up ~0.01% by weight; however, their importance in a number of processes cannot be overstated.[2]

Nature is limited to the use of bio-available metal ions, which explains, in part, the wide number of first row metals found in exemplary biological processes. However, many biomolecules are well-suited to interact with rarer second and third row transition metals, which can elicit novel biological responses. A well-known example of a metal-based medicinal complex is cisplatin (**1**; Figure 1).[3] The natural abundance, or lack thereof, of Pt explains its absence in natural systems. That said, its widespread application as an anticancer drug in the form of *cis*-$Pt(NH_3)_2Cl_2$ and analogous Pt(II) complexes is a testament to the relevance of late-metal ions in biology[4] and has motivated numerous searches for new metalloanticancer drugs.[5] Organometallic complexes represent a growing subset of potential anticancer drug molecules,[6] with certain arene-Ru compounds showing high activity as antiproliferative agents, such as Ru(*p*-cymene)(pta)Cl_2 (**2**; Figure 1; pta = 1,3,5-triaza-phosphaadamantane).[7] While biological applications of metal ions are certainly not limited to anticancer drug development, these hallmark Pt(II) and arene Ru investigations have motivated the use of coordination-driven self-assembly to form new biologically relevant materials due to the widespread use of both metal centers in the formation of supramolecular coordination complexes.

The use of metal-ligand bonding to drive the formation of metal-organic materials has been exploited in a number of synthetic strategies,[8] furnishing a variety of related but structurally diverse species dominated by metal-organic frameworks (MOFs)[9] and supramolecular coordination complexes (SCCs).[10] Methods to form the latter are aptly described as *coordination-driven self-assembly*, reflecting that formation occurs from mixtures containing donor (metal) and acceptor (ligand) precursors, ideally generating unique discrete structures with metal-ligand bonding as the impetus.[8,10]

The motivation for applying SCCs towards biological applications stems from a number of their inherent properties. First, the dimensions of a metallacycle or cage may be readily tuned without significant synthetic changes. Second, the specific metal ion used is versatile since coordination geometries are oftentimes predictable for a given element in a controllable oxidation state. Third, coordination-driven self-assembly allows for the incorporation of functional groups through pre-or post-self-assembly modifications.[11] Finally, the internal cavity of SCCs manifests host/guest capabilities which provide promise for sensing applications[12] as well as drug-delivery scaffolds,[13] especially given the evidence that nanoscopic materials may show selective uptake in cancerous cells due to increased permeability.[14]

NIH-PA Author Manuscript

NIH-PA Author Manuscript

NIH-PA Author Manuscript

Ruthenium SCCs as Anticancer Agents

In 1992, Tocher and coworkers reported the first studies of an arene-ruthenium complex acting as an anticancer agent.[15] The small drug molecule, Ru(η6-C_6H_6) (metronidazole)Cl_2 (**3**; Figure 2; metronidazole = 1-hydroxyethyl-2-methyl-5-nitroimidazole), incorporated the existing metronidazole antibiotic as the third ligand on a simple piano-stool Ru center. Interestingly, the selective cytotoxicity of complex **3** exceeded that of free metronidazole, illustrating that the inclusion of metal centers into a material can enhance the activity of existing drugs.

The latter strategy, utilizing host/guest chemistry to deliver a drug molecule, was described in an early biological application of SCCs by Therrien and coworkers[16] which utilized the self-assembly of *p*-cymeneruthenium-based metal fragments with pyridyl donors, as pioneered in 1997 by Süss-Fink and coworkers.[17] In this study, a trigonal prism was assembled by cofacially orienting two tritopic tripyridyl ligands with three diruthenium molecular clips. By combining clip **4** with a 1,3,5-substituted triazine (**5**; Figure 3) in the presence of AgOTf, a [3 + 2] self-assembly occurred with simultaneous anion exchange to furnish $[Ru_6(p\text{-}^{i}PrC_6H_4Me)_6(tpt)(dobq)_3]^{6+}$ (**SCC1**; tpt = 2,4,6-tris(pyridin-4-yl)-1,3,5-trizaine, dobq = 2,5-dioxydo-1,4-benzoquinonato). The trigonal prism was capable of encapsulating [(acac)M_2] (M = Pd, Pt; acac=acetylacetonato) and the anticancer activities of the host/guest ensembles were compared to the prism and free guest molecules. The IC_{50} values were determined using A2780 human ovarian cancer cells and revealed that **SCC1** (IC_{50} = 23 μM) was less effective than both the Pt and Pd host/guest ensembles (IC_{50} = 12 and 1 μM respectively), whereas the free [(acac)M_2] species were inactive. These results were rationalized by the observation that both [(acac)Pt_2] and [(acac)Pd_2] are insoluble in water and can only undergo cell-uptake encapsulated by the more-soluble trigonal prism. Subsequent release from the prism allowed the now-active cytotoxic Pd and Pt species to act in addition to the Ru centers.

SCC1 was also subjected to reactivity studies to determine the effects of various biomolecules on the stability of Ru-based SCCs in biological environments.[18] ESI-MS and NMR were used to investigate the action of amino acids, ascorbic acid and glutathione on the cage. These studies revealed that certain amino acids, specifically arginine, histidine and lysine, all caused disassembly of **SCC1**, while methionine had no effect. Ascorbic acid and glutathione were catalytically oxidized, noted as a possible origin of cytotoxicity. These tests show the importance of carefully investigating the interactions of SCCs with biomolecules due to the potential for disassembly; mechanistic conclusions that invoke an intact SCC within an intercellular environment must be justified by stability experiments given the variety of decomposition vectors present.

Stang, Chi and coworkers also assessed the activity of three-dimensional Ru-based SCCs, detailing the [3 + 2] self-assembly of four novel trigonal prisms (Figure 4).[19] The ligand employed in these studies was 1,3,5-tris(pyridin-4-ylethynyl)benzene (**10**). In addition to a dobq-bridged molecular clip (**7**), three other diruthenium triflate salts were used, differing by their O,O∩O,O moieties, specifically oxalato (**6**),[17] 5,8-dioxydo-1,4-naphthoquinonato (donq; **8**), and 5,11-dioxydo-6,12-tetracenquinonato (dotq; **9**) bridges. Anticancer activity was established using five cell lines, SK-hep-1 (liver), HeLa (ovary), HCT-15 (colon), A-549 (lung), and MDA-MB-231 (breast). While the prisms containing the dobq and dotq spacers were inactive across all cell lines, the oxalate and donq-based scaffolds were active, especially in the case of **4** (Table 1).

These activities suggest that there is no correlation between cytotoxicity and the size of the aromatic system of the spacer ligand; the high activity of **SCC4** was absent in its dotq-

NIH-PA Author Manuscript

NIH-PA Author Manuscript

NIH-PA Author Manuscript

bridged counterpart. In addition, the dobq-based molecular clip, which was a component of the active **SCC1**, did not appear to manifest any anticancer properties in **SCC3**. These results highlight the importance of detailed mechanistic studies to isolate the factors associated with increased activity in order to guide future designs. For instance, a given ligand may provide the necessary dimensions for a particularly effective SCC, or may facilitate degradation to deliver active Ru-containing fragments, with the assembly acting as a prodrug.

While these pioneering studies indicate that trigonal prismatic cages may possess low IC_{50} values for particular combinations of donors and molecular clips, the most diverse subset of SCCs investigated for Ru-based anticancer activity are [2 + 2] self-assembly scaffolds. Early examples of [2 + 2] assemblies used in biological studies were given by Navarro, Barea and coworkers[20] and Therrien and coworkers.[21] The former report involved rigid dipyridyl-based ligands to form Ru metallacycles that underwent noncovalent binding with DNA and exhibited significantly different resistance factors to cisplatin. This result was taken as evidence for a different mode of action of the Ru SCCs versus Pt-based drugs.[20] The latter studies also used rigid dipyridyl ligands as well as pyrazine to bridge one of four Ru-clips. Biological assays revealed a range of toxicities for the eight metallacycles, ranging from 4 – 66 μM relative to the cisplatin control of 2 μM for A2780 ovarian cancer cells.[21]

Stang, Chi and coworkers have reported a suite of [2 + 2] SCCs, each formed using molecular clips (**6** – **9**) and pyridyl-based donor ligands. The most straightforward of these assemblies incorporate the 4-pyridyl building blocks depicted in Figure 5.[22] In vitro anticancer activities were assessed using four cancer cell lines, SK-hep-1 (liver), HeLa (ovarian), HCT-15 (colon), and AGS (gastric). Of the eleven SCCs investigated, seven exhibited activity, as summarized in Table 2. The IC_{50} values of the corresponding clips were significantly higher, with only the donq clip showing measurable activity for SK-hep-1 cells.[23] The donq-based SCCs were particularly potent, with IC_{50} values oftentimes exceeding that of cisplatin, and on par with a second control drug, doxorubicin. The oxalato and dobq-containing species were relatively inactive in comparison. While the dotq ligand was present in **SCC7**, which had low IC_{50} values, this activity was attributed not to the Ru-acceptor, but rather the Pt-containing donor ligand, **11**, which in combination with the donq molecular clip, **8**, gave by far the most active assembly, **SCC6**. In fact, this mixed-metal assembly had IC_{50} values lower than cisplatin for all four cell lines. Some evidence for heightened activity resulting from longer donors was found, with assemblies using the long diethynyl spacer showing some efficacy, however, it is not immediately clear if this was due to length or other factors, such as the solubility differences between ethynyl moieties versus phenyl spacers.

The increased efficacy observed with extended, diethynyl spacers was reproduced using related 3-pyridyl-based donors, 1,2-di(pyridin-3-yl)ethyne, **15** and 1,4-di(pyridin-3-yl)buta-1,3-diyne, **16**. [24] These two ligands were used with molecular clips **6** – **9** to form eight unique, distorted rectangular assemblies, **SCC17-SCC24** (Figure 5). For the assemblies containing **15**, only the donq-based system exhibited low IC_{50} values. The oxalato and dobq-based SCCs gave measureable cytotoxicities when combined with the longer diethynyl ligand, **16**. While the dotq-bridged SCC was slightly active with the shorter dipyridyl ligand (**SCC20**), the efficacy of the extended dotq assembly (**SCC24**) was much higher (Table 2). From these combined results, larger assemblies appeared to be more active than their shorter analogues, though the extent to which activity is directly affected by size versus indirect effects from size-dependent solubility differences and other factors warrants further investigation.

NIH-PA Author Manuscript

NIH-PA Author Manuscript

NIH-PA Author Manuscript

Related studies by Stang and Chi further expanded the library of biologically active SCCs. For example, by incorporating amide groups into the core of dipyridyl donors, **17** and **18**,[25] sites for hydrogen bonding were preserved and the presence of azo functionalities on donors **19**–**22** unlock potential photo-sensitization.[23] The assemblies formed from the combinations of **17**–**22** with **6**–**9** were investigated using five cell lines obtained from American Type Culture Collection for **SCC25-SCC27**: HeLa, HCT-15, and MDA-MB-231, SK-hep-1, A-549, with the latter two cell lines also used in assays with the sixteen azodipyridyl-based assemblies. **SCC25** and **SCC26**, containing the oxalate bridged clip, were inactive, while rectangle **SCC27**, which employed the donq-bridged clip, possessed IC_{50} values that were similar to those of cisplatin, with values (μM) of 4.2 ± 0.11 (SK-hep-1); 10.2 ± 0.21 (HeLa); 3.7 ± 0.10 (HCT-15); 3.2± 0.11(A-549); 2.8 ± 0.03 (MDA-MB-231). Similar results were found for the azodipyridyl SCCs, with significant cytotoxicities found only for the donq-containing assemblies (**SCC36-SCC39**) with IC_{50} values ranging from ~12 – 37 μM.

Another subset of [2 + 2] assemblies from Stang and Chi uses an asymmetric donor, *N*-(4-(pyridin-4-ylethynyl)phenyl)isonicotinamide (**23**).[26] The presence of two asymmetric ligands in a rectangular assembly results in two isomers based on their relative orientations (Figure 6). The head-to-head isomer (HTH) contains a mirror plane collinear with the ditopic donors that is absent in the head-to-tail isomer (HTT), being replaced by an inversion center. If no energetic preference exists, a statistical mixture is expected, which was the case when **23** was combined with clips **6** (oxalate) and **8** (donq). Once again, the rectangles formed using the donq-based clip had the lowest IC_{50} values (Table 3). While the molecular clip precursors were moderately active for some cell lines, in all cases their corresponding [2 + 2] assemblies showed lower IC_{50} values.

In addition to these cell viability studies, time-dependence of growth inhibition was investigated by preincubating the SCCs in a growth medium of 10% fetal bovine serum (FBS). The activity of **SCC45** decreased to 50% of its full efficacy after 24 hours, implicating the exogenous species present in FBS as responsible for the degradation.

Most recently, a new variant of molecular clip was employed wherein the metal centers were bridged by a bis-benzimidazole ligand.[27] This clip was combined with tritopic ligand **10** and ditopic **17** to form a [3 + 2] prism and a [2 + 2] rectangular metallacycle, respectively (Figure 7.). As summarized in Table 4, the IC_{50} values of the prism, **SCC46**, were particularly low as compared to the free molecular clip, the rectangle, and cisplatin, with the exception of assay run with A-549 cells in which the rectangle was most effective.

These studies establish that Ru-based SCCs fulfill multiple roles in the development of new anticancer treatments. First, the ability of 3D prisms to act as hosts for anticancer drugs allows unfavorable properties associated with the free drug molecules to be circumvented, such as low solubility. Host/guest chemistry also provides a method to protect drug molecules from degradation en route to their targets by shielding the molecules from the cellular environment. In addition, the arene-Ru moieties of these SCCs impart inherent activity, with IC_{50} values competitive with those determined for cisplatin and doxorubicin.

Metallosupramolecular Sensors

The internal cavities found in most 2D and 3D SCCs are well suited to act as receptor sites for small molecules. The careful selection of building blocks can impart a variety of useful properties, such as offering hydrogen bond donor and acceptor sites, tuning the hydrophobicity, spatial selection based on cavity size, etc. As such, the use of SCCs as sensors is a growing area of research.

NIH-PA Author Manuscript

NIH-PA Author Manuscript

NIH-PA Author Manuscript

Chi, Stang and coworkers described the synthesis and characterization of two arene-Ru-based SCCs formed via the [2 + 2] assembly of molecular clips **7** (dobq) and **9** (dotq) with the previously discussed diamide ligand, **17** (see Figure 8).[28] Absorption and emission titration studies revealed that **SCC48** exhibited minimal spectral changes when interacting with monoanionic species like halide anions or acetate. However, when rigid dianionic substrates were used, in this case the oxalate anion, noteworthy photophysical changes occured. As oxalate exchange disruption is a marker for a number of diseases, it is an important oxyanion in biology.[29]

The binding of oxalate was further probed by UV-vis titrations which indicated 1:1 stoichiometry. A Stern-Volmer constant of 5×10^4 M^{-1} was determined from photoluminescence titrations, indicative of a strong interaction between the SCC and oxalate. It was hypothesized that ground-state binding of oxalate to the amide receptor sites disrupted photoinduced electron transfer (PET) processes from the arene-Ru fragments which attenuated the quantum yield.

These results motivated further investigations using citrate and tartrate, two oxyanions that are relevant due to their role in a variety of biological processes.[30,31] Both substrates induced emission enhancements, with Stern-Volmer constants of 1.4×10^5 M^{-1} and 1.8×10^4 M^{-1}, for citrate and tartrate, respectively.

A follow-up study discussed the formation of so-called metalla-bowls which form via the [2 + 2] assembly of non-linear ditopic donors with molecular clips (Figure 10).[32] The spectral responses of **SCC50** were selective for the multicarboxylate anions oxalate, tartrate and citrate, with very little interaction with monoanions such as the halides, acetate and benzoate (Figure 11).

Similar UV-Vis and emission titration experiments were carried out with oxalate, furnishing a 1:1 binding model and Stern-Volmer constant of 1.5×10^4 M^{-1}. Tartrate and citrate anions also gave strong interactions; Stern-Volmer kinetic analysis of **SCC50** provided K_{sv} values of 1.9×10^4 M^{-1} and 2.7×10^4 M^{-1} for tartrate and citrate, respectively. These larger values relative to **SCC48** indicate that the three dimensional structures of arene-Ru-based assemblies play a role in their efficacies for binding substrates.

Metallacycle-DNA Interactions

Motivated in part by the interaction of zinc fingers with DNA and other biomolecules, Hannon and coworkers pioneered the self-assembly of bis(pyridylimine) ligands with metal ions to form metallosupramolecular cylinders.[33] The cylinders containing group 8 metals have been extensively studied and give rise to a number of DNA binding motifs. For instance, Fe-based cylinders can interact with the major grove of B-DNA, ultimately inducing coiling as characterized by circular and linear dichroism, microscopy and NMR experiments.[34] These same cylinders can recognize 3-way DNA junctions, particularly highlighting the noteworthy π-stacking, intercalation, H-bonding and other intermolecular interactions that can all occur simultaneously between a properly designed SCC and DNA constructs,[35] in some cases manifesting cytotoxicity without genotoxicity.[36] In keeping with the facile tunabilities associated with SCCs, impressive control over the helical chirality of these M_2L_3 constructs was illustrated by appending enantiopure arginine groups to the cylinders.[37] A second method for controlling chirality, established by Scott and coworkers, exploits ligands which give optically pure monomers. By tethering two such ligands into a ditopic building block, diastereomerically pure M_2L_3 assemblies are obtained. [38]

In 2007, these experiments were expanded to Ru analogues upon the discovery of suitable synthetic conditions to furnish $Ru_2(L)_3$ triple helicates (**SCC51**, Figure 12.). Like its Fe

NIH-PA Author Manuscript

NIH-PA Author Manuscript

NIH-PA Author Manuscript

counterpart, the Ru cylinder also bound and induced coiling in DNA and exhibited cytotoxicities (IC_{50} = 22, 53 μM) marginally higher than those of cisplatin (4.9, 28 μM) for HBL100 and T47D cell lines, respectively.[39] More recently, the Ru helicates were found to inhibit DNA transactions through in vitro PCR assays.[40] The extensive studies of Hannon and coworkers has also lead to the caveat that assays involving SCCs must be carefully conducted to avoid effects caused by incubation times or volumes, which can cause drastically different results for a single cell line, rendering single-point comparisons to cisplatin or other reference drugs potentially irrelevant.[41]

The stabilization of G-quadruplex motifs that form from the folding of G-rich sections of the single-stranded DNA telomere has been shown to inhibit the enzyme telomerase and the transcription activity of certain oncogenes. Since telomerase is active in ~87% of cancer cells, molecules which can stabilize G-quadruplex formation are potential anticancer agents. In 2008, Sleiman and coworkers recognized that a Pt-based SCC possessed many of the features predicted to afford strong G-quadruplex stabilization.[42] Computational models predicted that $[Pt(en)(4,4'\text{-bipy})]_4(NO_3)_8$ would have favorable binding to a 22-mer G-quadruplex structure (Figure 13). This model indicated that the ethylenediamine ligands were active in hydrogen bonding to phosphate oxygen atoms. Further stabilization was expected from interactions between the 4,4'-bpy rings and the guanine bases.

The binding was studied experimentally using a FRET melting assay which indicated a ΔT_m of 34.5°C (the shift in the thermal denaturation temperature) with 0.75 μM concentrations of **SCC52**. This stabilization slightly exceeded the values (27.5 – 33.8°C) of known binders, which were studied at 1 μM concentrations. An alternative measure of stabilization is the concentration required to achieve a ΔT_m of 20°C, which was found to be 0.40 μM for **SCC52**, again a very competitive value as compared to other known binders, which ranged from 0.38 to 0.70 μM.[42]

Studies of DNA stabilization by SCCs have since been extended to Ru-based assemblies. Vilar, Therrien and coworkers have shown that tetragonal prisms formed from tetrapyridyl porphyrin and a dobq-based clip will bind to both telomeric and *c-myc* DNA, albeit with little selectivity between duplex and quadruplex strands.[43]

SCCs containing Pt and Pd were also found to interact with supercoiled DNA based on studies by Chi, Stang and coworkers.[44] The specific SCCs studied were heterobimetallic in nature due to the use of a ferrocenyl diphosphine ligand used to cap *cis* sites of the Pd and Pt precursors (**27** and **28**, respectively). [2 + 2] assembly of the metal precursors with the previously discussed non-linear ditopic diamide dipyridyl ligand (**25**) furnished two rhomboid-like SCCs (Figure 14). Initial investigations of **SCC53** and **SCC54** with DNA used photophysical characterization. Both rhomboids displayed spectral changes upon titration of DNA into solution, with hypochromic shifts occurring throughout all absorption features. The corresponding K_{sv} values from emission titrations were 3.86×10^3 M^{-1} (**SCC53**) and 2.14×10^3 M^{-1} (**SCC54**), indicating significant fluorescence quenching in the presence of DNA.

The SCC/DNA interaction was further explored using gel electrophoresis which showed that both **SCC53** and **SCC54** were effective at unraveling supercoiled pUC19 DNA samples. While the Pd-based SCC was determined to have a higher binding constant, the electrophoresis studies indicated that the Pt-based rhomboid was better at unwinding the pUC19 sample, which was further corroborated by CD experiments in which a 50% decrease in the positive bands was observed commensurate with a blue-shift in wavelengths. Neither the donor nor acceptor precursors showed positive DNA unwinding.

NIH-PA Author Manuscript

NIH-PA Author Manuscript

NIH-PA Author Manuscript

Metallacycle-Protein Interactions

There has been growing interest in targeting proteins in the development of new drugs. Sava and coworkers put forth the caveat that the dominant focus on DNA as a target for the development of new drugs and the exploration of mechanistic pathways may hinder the discovery of new anticancer agents.[45] To support this, they highlight the lack of understanding of DNA-adduct formation and efficacy of certain Pt-based anticancer drugs with specific tumor types.[46,47] In addition, they reinforce the contradiction between the development of cisplatin resistance and the expression of DNA repair systems while pointing out that a correlation has been observed between the function of p35 mutant proteins and the activity of cisplatin.[48] A mini-review by Casini and Reedijk[49] discusses examples of in vitro studies of existing Pt-based drugs provided clear evidence that these compounds are capable of interacting with proteins, sometimes affecting the mechanism of action.[50]

A study by Qu and coworkers describes the use of triple-helical supramolecular cylinders which inhibit β-amyloid aggregation with implications for the treatment of Alzheimer's disease.[51] These cylindrical SCCs are of the type used by Hannon and coworkers in their studies of DNA interactions (Figure 15).[33,52]

The Fe-based **SCC56** exhibited stronger inhibition over its Ni counterpart (**SC55**) using a fluorescence Aβ-ECFP fusion assay. In addition to inhibiting aggregation, the cytotoxicity of both SCCs was evaluated using an MTT assay. When treated with Aβ1-40, a decrease of 53% was observed, which could be prevented upon addition of the Ni or Fe SCC. When the complexes were used in the absence of Aβ1-40, no effect was observed, implicating complex binding as an important mechanistic step. Further studies using rat models indicated that the compounds were effective in curing spatial memory defects induced by hyperchomocysteinemia. This work is the first example of aggregation inhibition by SCCs and is a noteworthy proof-of-concept of the biological relevance that such compounds possess.

Conclusion

While the biological application of SCCs is still an emergent field of study, with the examples discussed here all based on publications only dating as far back as 2008, these pioneering results confirm supramolecular scaffolds have impressive relevance to a wide variety of biochemical and biomedical targets. Individual building blocks can be used to construct multifunctional SCCs, which in some cases can exhibit anticancer activity, act as selective sensors for biologically important analytes, and can interact with DNA and proteins. Due to the myriad of possible SCCs and the almost limitless modularity and tunability afforded without significant synthetic penalty, the biological applications of such species is expect to continue along this already promising path.

Acknowledgments

P.J.S. thanks the U.S. National Institutes of Health (NIH; Grant GM-057052) for financial support. K.W.C gratefully acknowledges financial support from the World Class University (WCU) program (R33-2008-000-10003) and Priority Research Centers program (2009-0093818) through the National Research Foundation of Korea (NRF).

NIH-PA Author Manuscript

NIH-PA Author Manuscript

NIH-PA Author Manuscript

Biography

Timothy R. Cook received his B.A. degree from Boston University and his Ph.D. from the Massachusetts Institute of Technology. In 2010, he joined the Stang Group at Utah as a postdoc and later as an assistant research professor.

Vaishali Vajpayee obtained her Ph.D. from University of Rajasthan. In 2008, she joined the Chi Group as postdoc at Ulsan. In 2012, she moved to the University of Angers working with Prof Marc Sallé.

Min Hyung Lee received B.S. and Ph.D. degrees from the Korea Advanced Institute of Science and Technology. He is currently an associate professor of chemistry in the University of Ulsan, Republic of Korea.

Peter J. Stang is a Distinguished Professor of Chemistry at Utah; a member of the US National Academy of Sciences; the American Academy of Arts and Sciences and the 2012 recipient of the ACS Priestley Medal.

Ki-Whan Chi received a Ph.D. degree from the University of Washington. He is currently a professor and the leader of BK21 and WCU projects in the Department of Chemistry, University of Ulsan.

REFERENCES

1. Kraatz, H-B.; Metzler-Nolte, N. Concepts and models in bioinorganic chemistry. Wiley-VCH: Weinheim; 2006.
2. Bhattacharya, PK. Metal Ions in Biochemistry. Alpha Science International Limited; 2005.
3. Sherman SE, Lippard SJ. Structural aspects of platinum anticancer drug interactions with DNA. Chem. Rev. 1987; 87:1153–1181.
4. Jung Y, Lippard SJ. Direct Cellular Responses to Platinum-Induced DNA Damage. Chem. Rev. 2007; 107:1387–1407. [PubMed: 17455916]
5. Kelland L. The resurgence of platinum-based cancer chemotherapy. Nat. Rev. Cancer. 2007; 7:573–584. [PubMed: 17625587]
6. Jaouen, G. Bioorganometallics: Biomolecules, Labeling, Medicine. John Wiley & Sons; 2006.
7. Chatterjee S, Kundu S, Bhattacharyya A, Hartinger C, Dyson P. The ruthenium(II)–arene compound RAPTA-C induces apoptosis in EAC cells through mitochondrial and p53–JNK pathways. JBIC Journal of Biological Inorganic Chemistry. 2008; 13:1149–1155.
8. Cook TR, Zheng Y-R, Stang PJ. Metal-Organic Frameworks and Self-Assembled Supramolecular Coordination Complexes: Comparing and Contrasting the Design, Synthesis, and Functionality of Metal-Organic Materials. Chem. Rev. 2013; 113:734–777. [PubMed: 23121121]
9. James SL. Metal-organic frameworks. Chem. Soc. Rev. 2003; 32:276–288. [PubMed: 14518181]
10. Chakrabarty R, Mukherjee PS, Stang PJ. Supramolecular Coordination: Self-Assembly of Finite Two- and Three-Dimensional Ensembles. Chem. Rev. 2011; 111:6810–6918. [PubMed: 21863792]
11. Wang M, Lan W-J, Zheng Y-R, Cook TR, White HS, Stang PJ. Post-Self-Assembly Covalent Chemistry of Discrete Multicomponent Metallosupramolecular Hexagonal Prisms. J. Am. Chem. Soc. 2011; 133:10752–10755. [PubMed: 21671637]
12. Wang M, Vajpayee V, Shanmugaraju S, Zheng Y-R, Zhao Z, Kim H, Mukherjee PS, Chi K-W, Stang PJ. Coordination-Driven Self-Assembly of M3L2 Trigonal Cages from Preorganized Metalloligands Incorporating Octahedral Metal Centers and Fluorescent Detection of Nitroaromatics. Inorg. Chem. 2011; 50:1506–1512. [PubMed: 21214171]
13. Therrien, B. Drug Delivery by Water-Soluble Organometallic Cages. In: Albrecht, M.; Hahn, E., editors. Chemistry of Nanocontainers. Vol. Vol. 319. Springer Berlin Heidelberg; 2011. p. 35-55.

NIH-PA Author Manuscript NIH-PA Author Manuscript NIH-PA Author Manuscript

14. Matsumura Y, Maeda H. A New Concept for Macromolecular Therapeutics in Cancer Chemotherapy: Mechanism of Tumoritropic Accumulation of Proteins and the Antitumor Agent Smancs. Cancer Res. 1986; 46:6387–6392. [PubMed: 2946403]
15. Dale LD, Tocher JH, Dyson TM, Edwards DI, Tocher DA. Studies on DNA Damage and Induction of SOS Repair by Novel Multifunctional Bioreducible Compounds. II. A Metronidazole Adduct of a Ruthenium-arene Compound. Anti-Cancer Drug Design. 1992; 7:3–14. [PubMed: 1543526]
16. Therrien B, Süss-Fink G, Govindaswamy P, Renfrew AK, Dyson PJ. The "Complex-in-a-Complex" Cations [(acac)2M⊂Ru6(p-iPrC6H4Me)6(tpt)2(dhbq)3]6+: A Trojan Horse for Cancer Cells. Angew. Chem. Int. Ed. 2008; 47:3773–3776.
17. Yan H, Suss-Fink G, Neels A, Stoeckli-Evans H. Mono-, di- and tetra-nuclear p-cymeneruthenium complexes containing oxalato ligands. Journal of the Chemical Society, Dalton Transactions. 1997; 0:4345–4350.
18. Paul LEH, Therrien B, Furrer J. Investigation of the Reactivity between a Ruthenium Hexacationic Prism and Biological Ligands. Inorg. Chem. 2011; 51:1057–1067. [PubMed: 22221272]
19. Vajpayee V, Yang YJ, Kang SC, Kim H, Kim IS, Wang M, Stang PJ, Chi K-W. Hexanuclear self-assembled arene-ruthenium nano-prismatic cages: potential anticancer agents. Chem. Commun. 2011; 47:5184–5186.
20. Linares, Ft; Galindo, MA.; Galli, S.; Romero, MA.; Navarro, JAR.; Barea, E. Tetranuclear Coordination Assemblies Based on Half-Sandwich Ruthenium(II) Complexes: Noncovalent Binding to DNA and Cytotoxicity. Inorg. Chem. 2009; 48:7413–7420. [PubMed: 19586019]
21. Mattsson J, Govindaswamy P, Renfrew AK, Dyson PJ, Stepnicka P, Suss-Fink G, Therrien B. Synthesis, Molecular Structure, and Anticancer Activity of Cationic Arene Ruthenium Metallarectangles. Organometallics. 2009; 28:4350–4357.
22. Vajpayee V, Song YH, Yang YJ, Kang SC, Cook TR, Kim DW, Lah MS, Kim IS, Wang M, Stang PJ, Chi K-W. Self-Assembly of Cationic, Hetero-or Homonuclear Ruthenium(II) Macrocyclic Rectangles and Their Photophysical, Electrochemical, and Biological Studies. Organometallics. 2011; 30:6482–6489. [PubMed: 22180698]
23. Vajpayee V, Lee S, Kim S-H, Kang SC, Cook TR, Kim H, Kim DW, Verma S, Lah MS, Kim IS, Wang M, Stang PJ, Chi K-W. Self-assembled metalla-rectangles bearing azodipyridyl ligands: synthesis, characterization and antitumor activity. Dalton Trans. 2013; 42:466–475. [PubMed: 23073144]
24. Vajpayee V, Song YH, Jung YJ, Kang SC, Kim H, Kim IS, Wang M, Cook TR, Stang PJ, Chi K-W. Coordination-driven self-assembly of ruthenium-based molecular-rectangles: Synthesis, characterization, photo-physical and anticancer potency studies. Dalton Trans. 2012; 41:3046–3052. [PubMed: 22278716]
25. Vajpayee V, Song YH, Yang YJ, Kang SC, Kim H, Kim IS, Wang M, Stang PJ, Chi K-W. Coordination-Driven Self-Assembly and Anticancer Activity of Molecular Rectangles Containing Octahedral Ruthenium Metal Centers. Organometallics. 2011; 30:3242–3245. [PubMed: 21779140]
26. Mishra A, Jung H, Park JW, Kim HK, Kim H, Stang PJ, Chi K-W. Anticancer Activity of Self-Assembled Molecular Rectangles via Arene-Ruthenium Acceptors and a New Unsymmetrical Amide Ligand. Organometallics. 2012; 31:3519–3526. [PubMed: 22639481]
27. Vajpayee V, Lee Sm, Park JW, Dubey A, Kim H, Cook TR, Stang PJ, Chi K-W. Growth Inhibitory Activity of a Bis-Benzimidazole-Bridged Arene Ruthenium Metalla-Rectangle and -Prism. Organometallics. 2013; 32:1563–1566. [PubMed: 23580795]
28. Vajpayee V, Song YH, Lee MH, Kim H, Wang M, Stang PJ, Chi K-W. Self-Assembled Arene-Ruthenium-Based Rectangles for the Selective Sensing of Multi-Carboxylate Anions. Chem. Eur. J. 2011; 17:7837–7844. [PubMed: 21611989]
29. Morakot N, Rakrai W, Keawwangchai S, Kaewtong C, Wanno B. Design and synthesis of thiourea based receptor containing naphthalene as oxalate selective sensor. J Mol Model. 2010; 16:129–136. [PubMed: 19521724]
30. Pal R, Parker D, Costello LC. A europium luminescence assay of lactate and citrate in biological fluids. Org. Biomol. Chem. 2009; 7:1525–1528. [PubMed: 19343236]

NIH-PA Author Manuscript

NIH-PA Author Manuscript

NIH-PA Author Manuscript

31. Costello LC, Franklin RB. Prostatic fluid electrolyte composition for the screening of prostate cancer: a potential solution to a major problem. Prostate Cancer Prostatic Dis. 2008; 12:17–24. [PubMed: 18591961]
32. Mishra A, Vajpayee V, Kim H, Lee MH, Jung H, Wang M, Stang PJ, Chi K-W. Self-assembled metalla-bowls for selective sensing of multi-carboxylate anions. Dalton Trans. 2012; 41:1195–1201. [PubMed: 22116403]
33. Hannon MJ, Painting CL, Jackson A, Hamblin J, Errington W. An inexpensive approach to supramolecular architecture. Chem. Commun. 1997:1807–1808.
34. Hannon MJ, Moreno V, Prieto MJ, Moldrheim E, Sletten E, Meistermann I, Isaac CJ, Sanders KJ, Rodger A. Intramolecular DNA Coiling Mediated by a Metallo-Supramolecular Cylinder. Angew. Chem. Int. Ed. 2001; 40:879–884.
35. Oleksi A, Blanco AG, Boer R, Usón I, Aymamí J, Rodger A, Hannon MJ, Coll M. Molecular Recognition of a Three-Way DNA Junction by a Metallosupramolecular Helicate. Angew. Chem. Int. Ed. 2006; 45:1227–1231.
36. Hotze ACG, Hodges NJ, Hayden RE, Sanchez-Cano C, Paines C, Male N, Tse M-K, Bunce CM, Chipman JK, Hannon MJ. Supramolecular Iron Cylinder with Unprecedented DNA Binding Is a Potent Cytostatic and Apoptotic Agent without Exhibiting Genotoxicity. Chem. Biol. 2008; 15:1258–1267. [PubMed: 19101470]
37. Cardo L, Sadovnikova V, Phongtongpasuk S, Hodges NJ, Hannon MJ. Arginine conjugates of metallo-supramolecular cylinders prescribe helicity and enhance DNA junction binding and cellular activity. Chem. Commun. 2011; 47:6575–6577.
38. Howson SE, Bolhuis A, Brabec V, Clarkson GJ, Malina J, Rodger A, Scott P. Optically pure, water-stable metallo-helical ‘flexicate’ assemblies with antibiotic activity. Nat Chem. 2012; 4:31–36. [PubMed: 22169869]
39. Pascu GI, Hotze ACG, Sanchez-Cano C, Kariuki BM, Hannon MJ. Dinuclear Ruthenium(II) Triple-Stranded Helicates: Luminescent Supramolecular Cylinders That Bind and Coil DNA and Exhibit Activity against Cancer Cell Lines. Angew. Chem. Int. Ed. 2007; 46:4374–4378.
40. Ducani C, Leczkowska A, Hodges NJ, Hannon MJ. Noncovalent DNA-Binding Metallo-Supramolecular Cylinders Prevent DNA Transactions in vitro. Angew. Chem. Int. Ed. 2010; 49:8942–8945.
41. Pope AJ, Bruce C, Kysela B, Hannon MJ. Issues surrounding standard cytotoxicity testing for assessing activity of non-covalent DNA-binding metallo-drugs. Dalton Trans. 2010; 39:2772–2774. [PubMed: 20200702]
42. Kieltyka R, Englebienne P, Fakhoury J, Autexier C, Moitessier N, Sleiman HF. A Platinum Supramolecular Square as an Effective G-Quadruplex Binder and Telomerase Inhibitor. J. Am. Chem. Soc. 2008; 130:10040–10041. [PubMed: 18616250]
43. Barry NPE, Abd Karim NH, Vilar R, Therrien B. Interactions of ruthenium coordination cubes with DNA. Dalton Trans. 2009; 0:10717–10719. [PubMed: 20023899]
44. Mishra A, Ravikumar S, Hong SH, Kim H, Vajpayee V, Lee H, Ahn B, Wang M, Stang PJ, Chi K-W. DNA Binding and Unwinding by Self-Assembled Supramolecular Heterobimetallacycles. Organometallics. 2011; 30:6343–6346. [PubMed: 22180697]
45. Sava G, Jaouen G, Hillard EA, Bergamo A. Targeted therapy vs. DNA-adduct formation-guided design: thoughts about the future of metal-based anticancer drugs. Dalton Trans. 2012; 41:8226–8234. [PubMed: 22614531]
46. Sonpavde G, Sternberg CN. Satraplatin for the therapy of castration-resistant prostate cancer. Future Oncology. 2009; 5:931–940. [PubMed: 19792961]
47. Sanborn R. Cisplatin Versus Carboplatin in NSCLC: Is There One “Best” Answer? Current Treatment Options in Oncology. 2008; 9:326–342. [PubMed: 19225891]
48. Perrone F, Bossi P, Cortelazzi B, Locati L, Quattrone P, Pierotti MA, Pilotti S, Licitra L. TP53 Mutations and Pathologic Complete Response to Neoadjuvant Cisplatin and Fluorouracil Chemotherapy in Resected Oral Cavity Squamous Cell Carcinoma. Journal of Clinical Oncology. 2010; 28:761–766. [PubMed: 20048189]
49. Casini A, Reedijk J. Interactions of anticancer Pt compounds with proteins: an overlooked topic in medicinal inorganic chemistry? Chemical Science. 2012; 3:3135–3144.

NIH-PA Author Manuscript

NIH-PA Author Manuscript

NIH-PA Author Manuscript

50. Che C-M, Siu F-M. Metal complexes in medicine with a focus on enzyme inhibition. Curr. Opin. Chem. Biol. 2010; 14:255–261. [PubMed: 20018553]

51. Yu H, Li M, Liu G, Geng J, Wang J, Ren J, Zhao C, Qu X. Metallosupramolecular complex targeting an [small alpha]/[small beta] discordant stretch of amyloid [small beta] peptide. Chemical Science. 2012; 3:3145–3153.

52. Kerckhoffs JMCA, Peberdy JC, Meistermann I, Childs LJ, Isaac CJ, Pearmund CR, Reudegger V, Khalid S, Alcock NW, Hannon MJ, Rodger A. Enantiomeric resolution of supramolecular helicates with different surface topographies. Dalton Trans. 2007:734–742. [PubMed: 17279244]

NIH-PA Author Manuscript

NIH-PA Author Manuscript

NIH-PA Author Manuscript

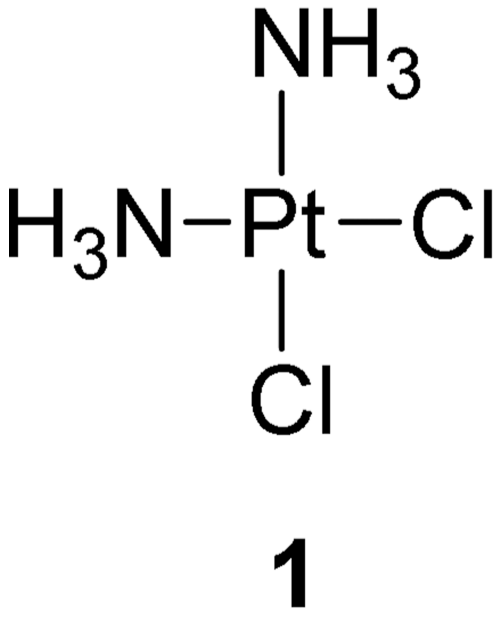

1

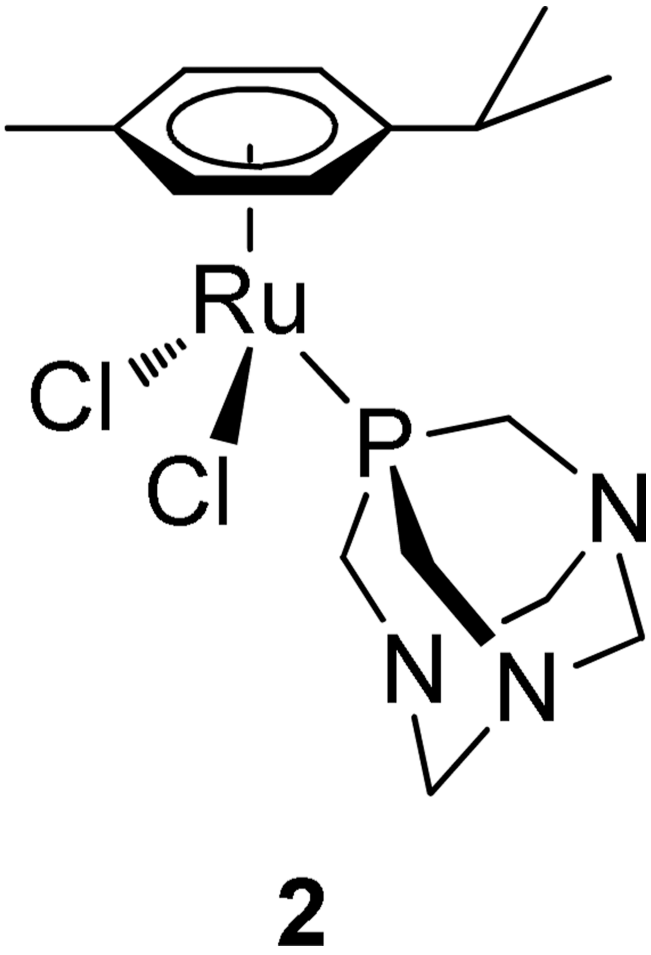

2

Figure 1.
Complexes based on Pt (cisplatin; **1**) and Ru (Ru(*p*-cymene)(pta)Cl_2; **2**) demonstrate the utility of second and third-row metals in biological applications.

NIH-PA Author Manuscript

NIH-PA Author Manuscript

NIH-PA Author Manuscript

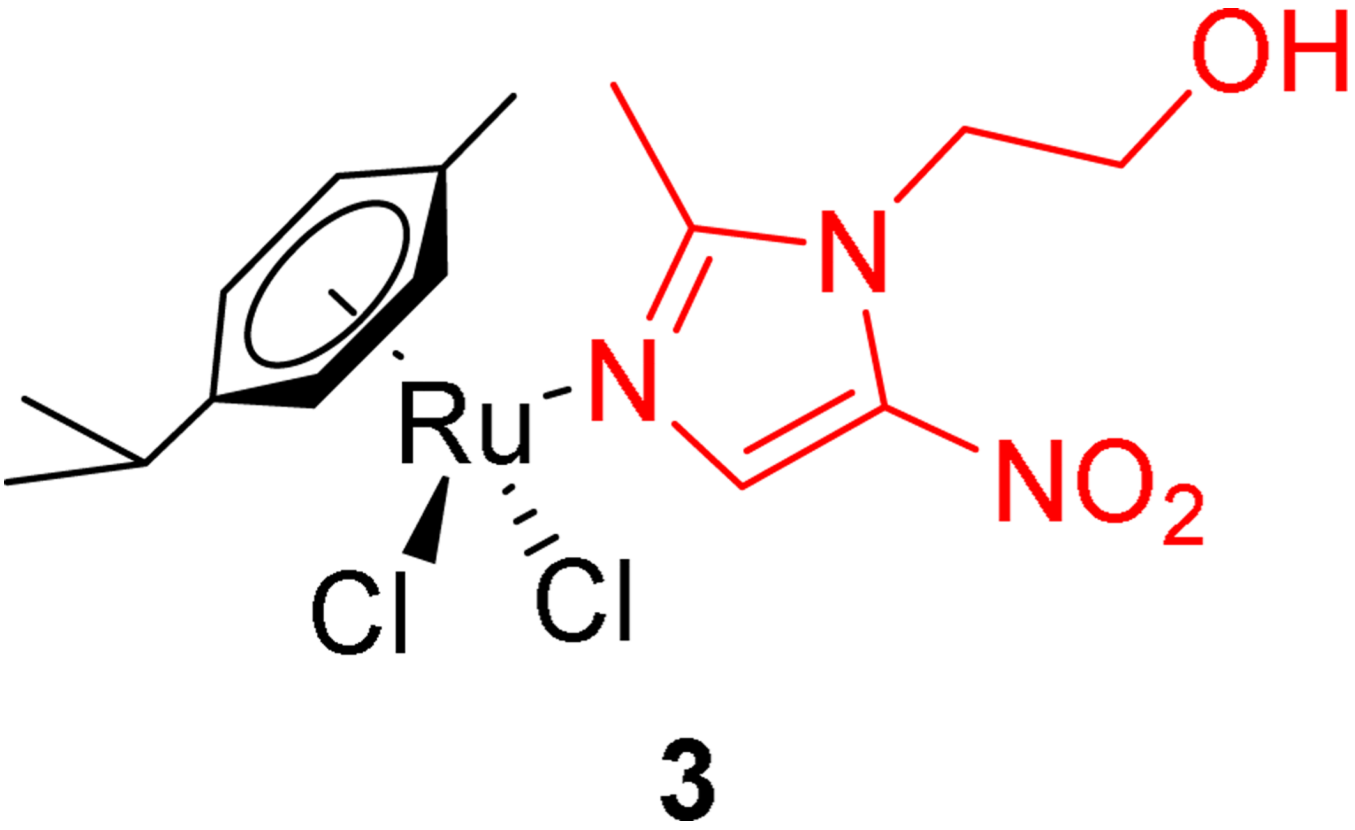

3

Figure 2.
The first metal-arene compound evaluated for anticancer activity. The ligand in red is the antibiotic agent metronidazole.

NIH-PA Author Manuscript

NIH-PA Author Manuscript

NIH-PA Author Manuscript

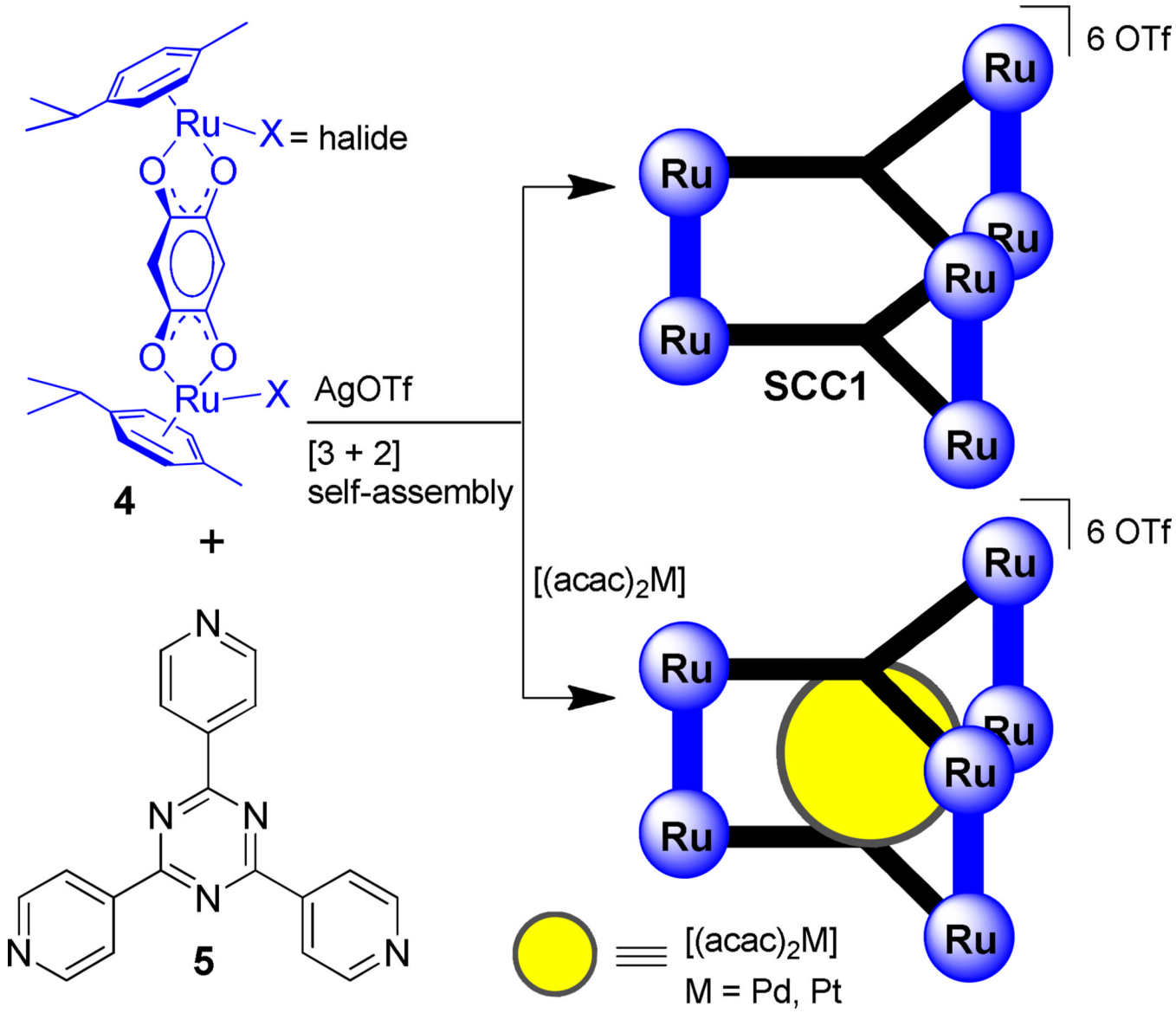

Figure 3.
The "Trojan Horse" SCC for anticancer drug delivery: a trigonal prismatic assembly with an internal cavity for host/guest chemistry.

NIH-PA Author Manuscript

NIH-PA Author Manuscript

NIH-PA Author Manuscript

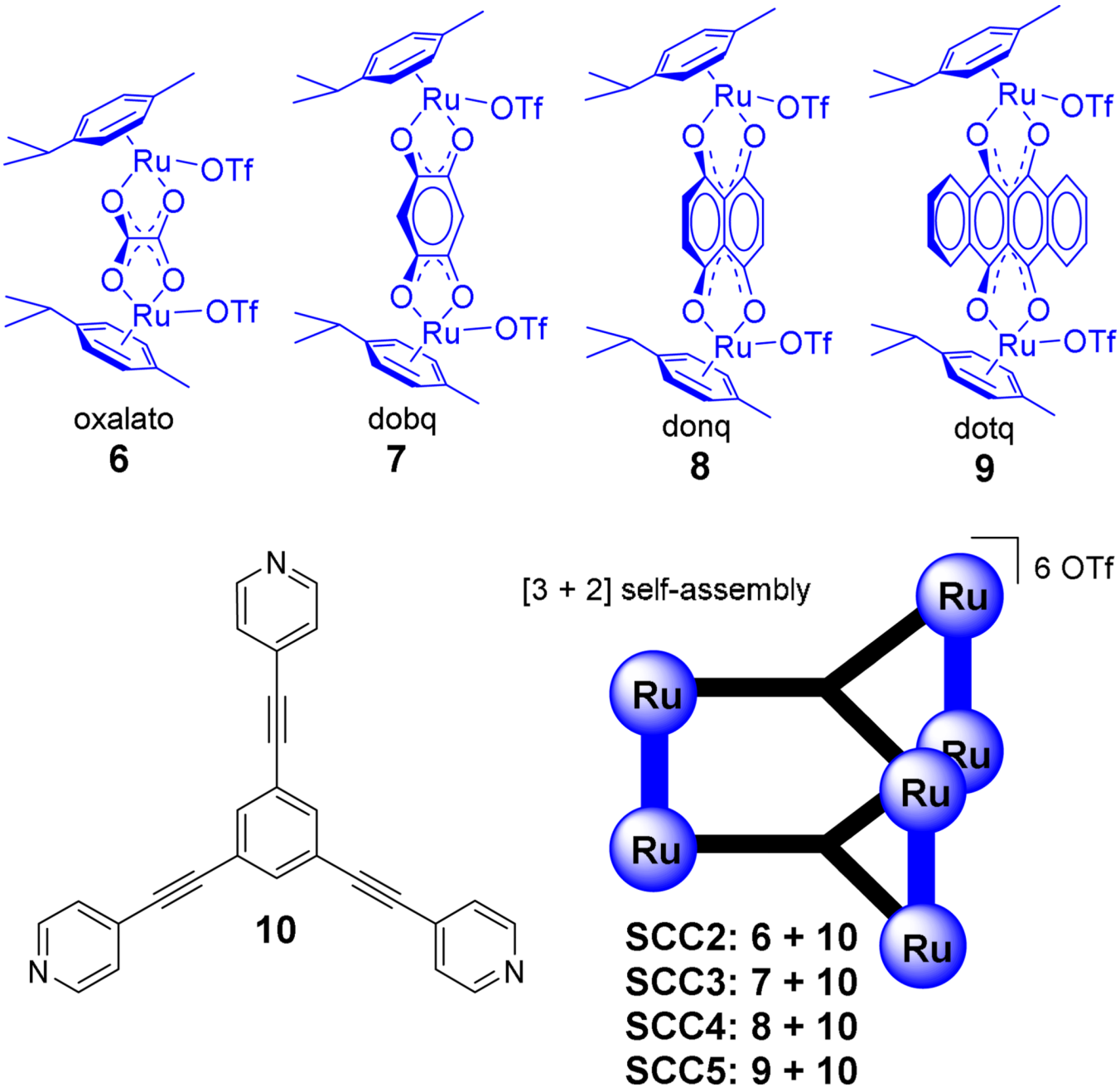

Figure 4.
Trigonal prisms are obtained from the [3 + 2] assembly of a tritopic planar ligand with molecular clips.

NIH-PA Author Manuscript

NIH-PA Author Manuscript

NIH-PA Author Manuscript

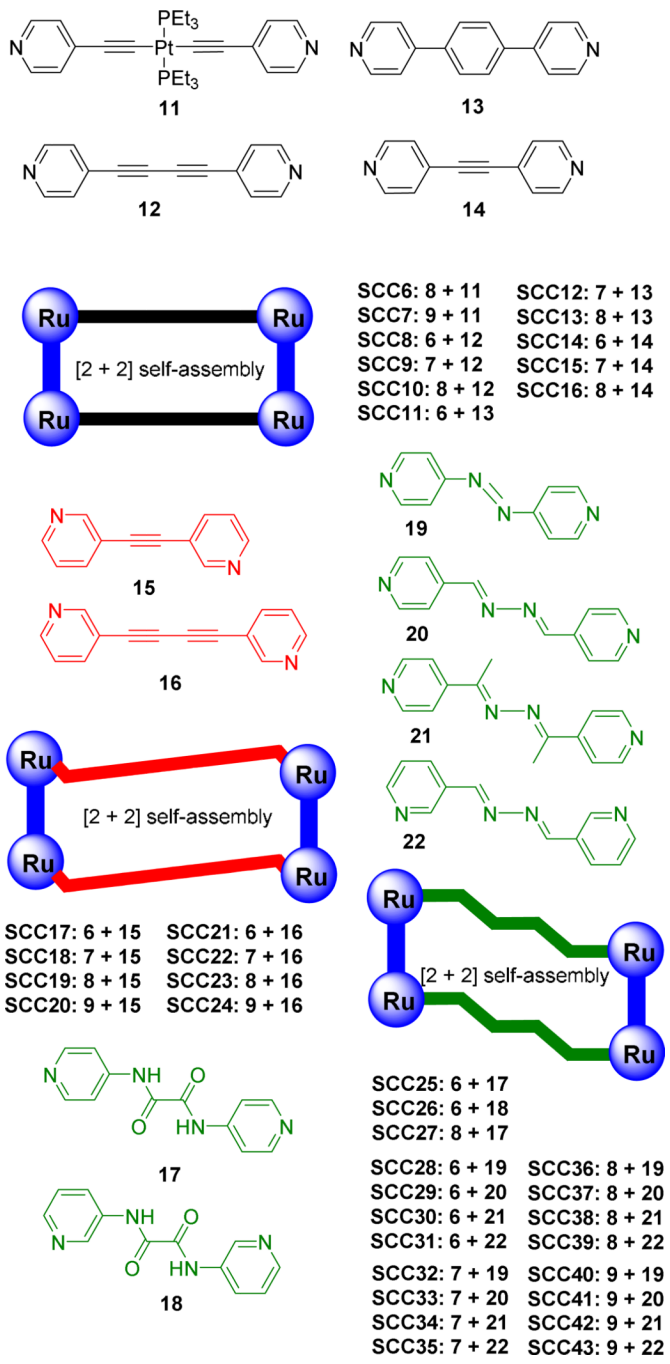

Figure 5.
Molecular clips **6 – 9** undergo [2 + 2] assembly with linear donors **11 – 22** to furnish unique metallacycles (**SCC6 – SCC43**).

NIH-PA Author Manuscript

NIH-PA Author Manuscript

NIH-PA Author Manuscript

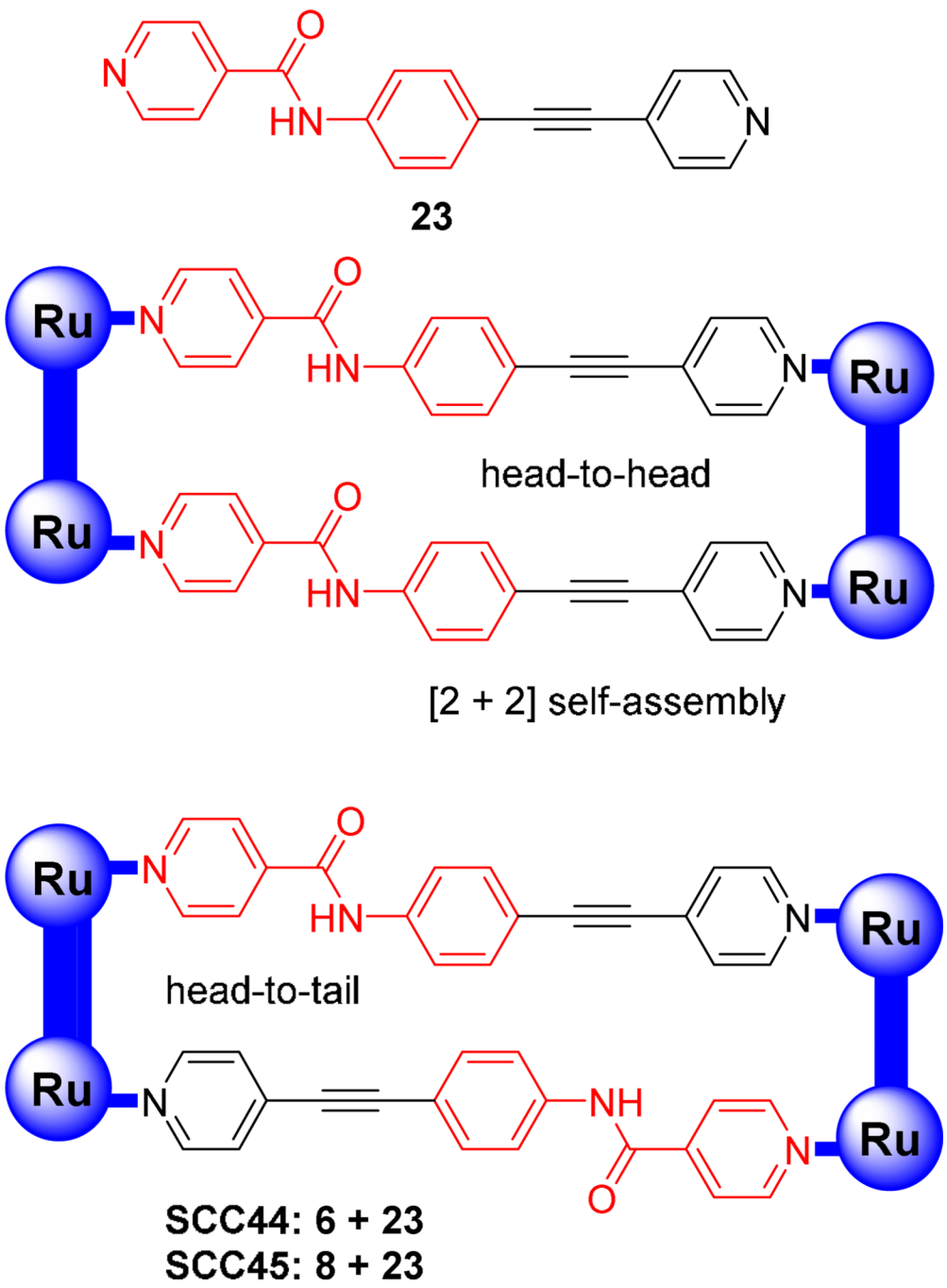

Figure 6.
The use of asymmetric ligands gives rise to two possible isomers, head-to-head and head-to-tail.

NIH-PA Author Manuscript

NIH-PA Author Manuscript

NIH-PA Author Manuscript

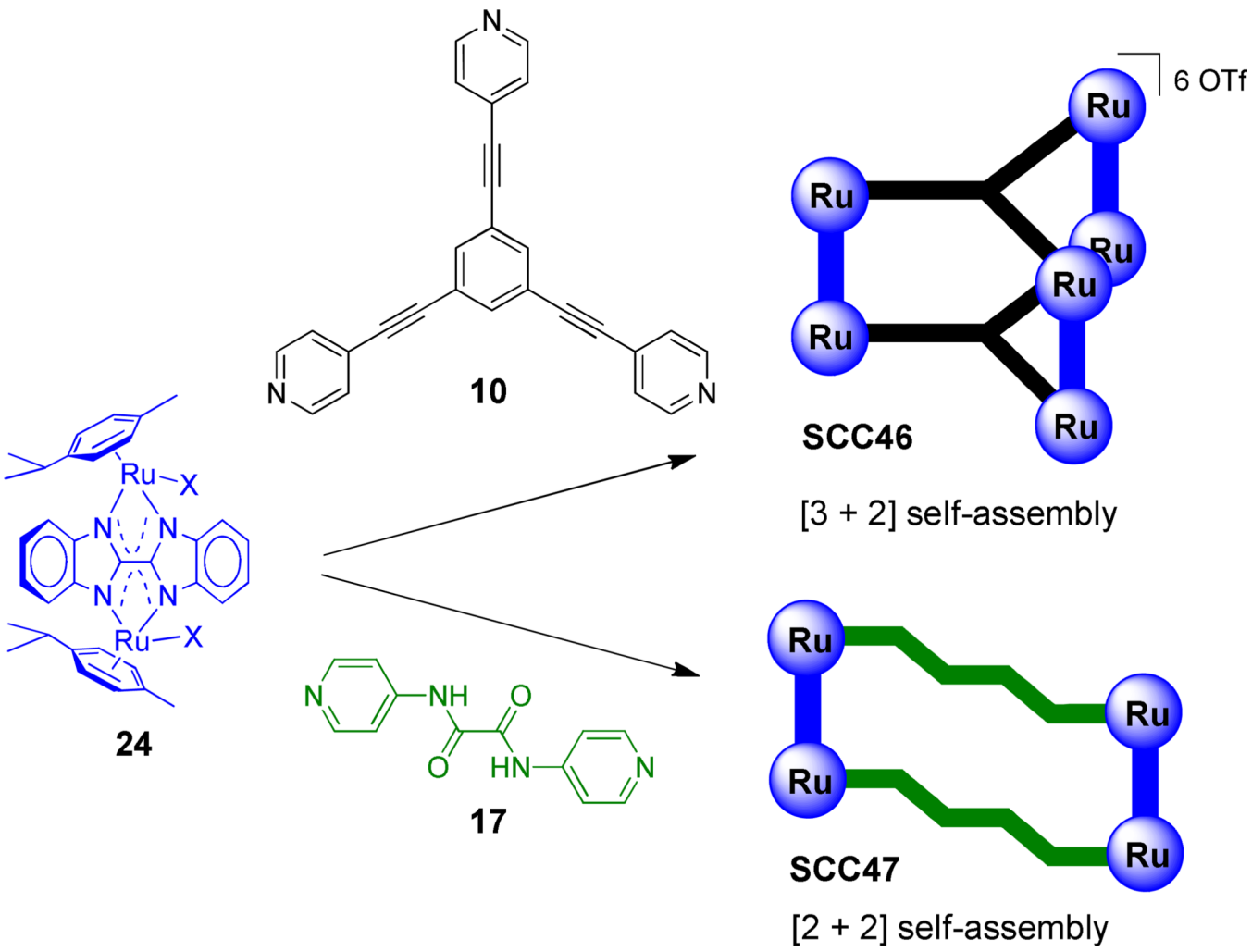

Figure 7.
Molecular clip **24** can be used to form a trigonal prism or a rectangular metallacycle.

NIH-PA Author Manuscript

NIH-PA Author Manuscript

NIH-PA Author Manuscript

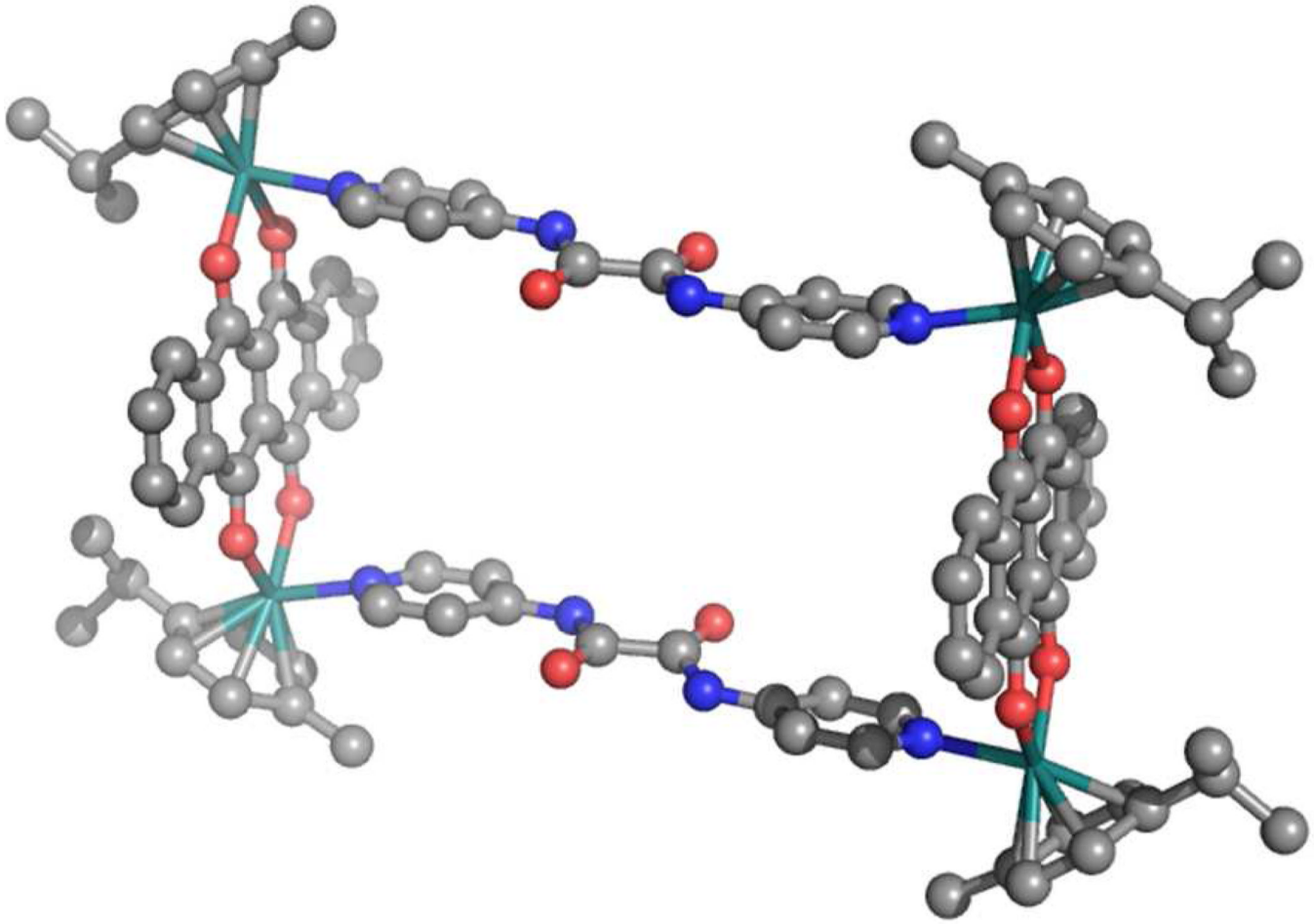

Figure 8.
X-ray crystal structure of **SCC48**. Hydrogen atoms, solvent molecules and counterions omitted for clarity. Atom (color): Ru (teal), N (blue), O (red), C (gray).

NIH-PA Author Manuscript

NIH-PA Author Manuscript

NIH-PA Author Manuscript

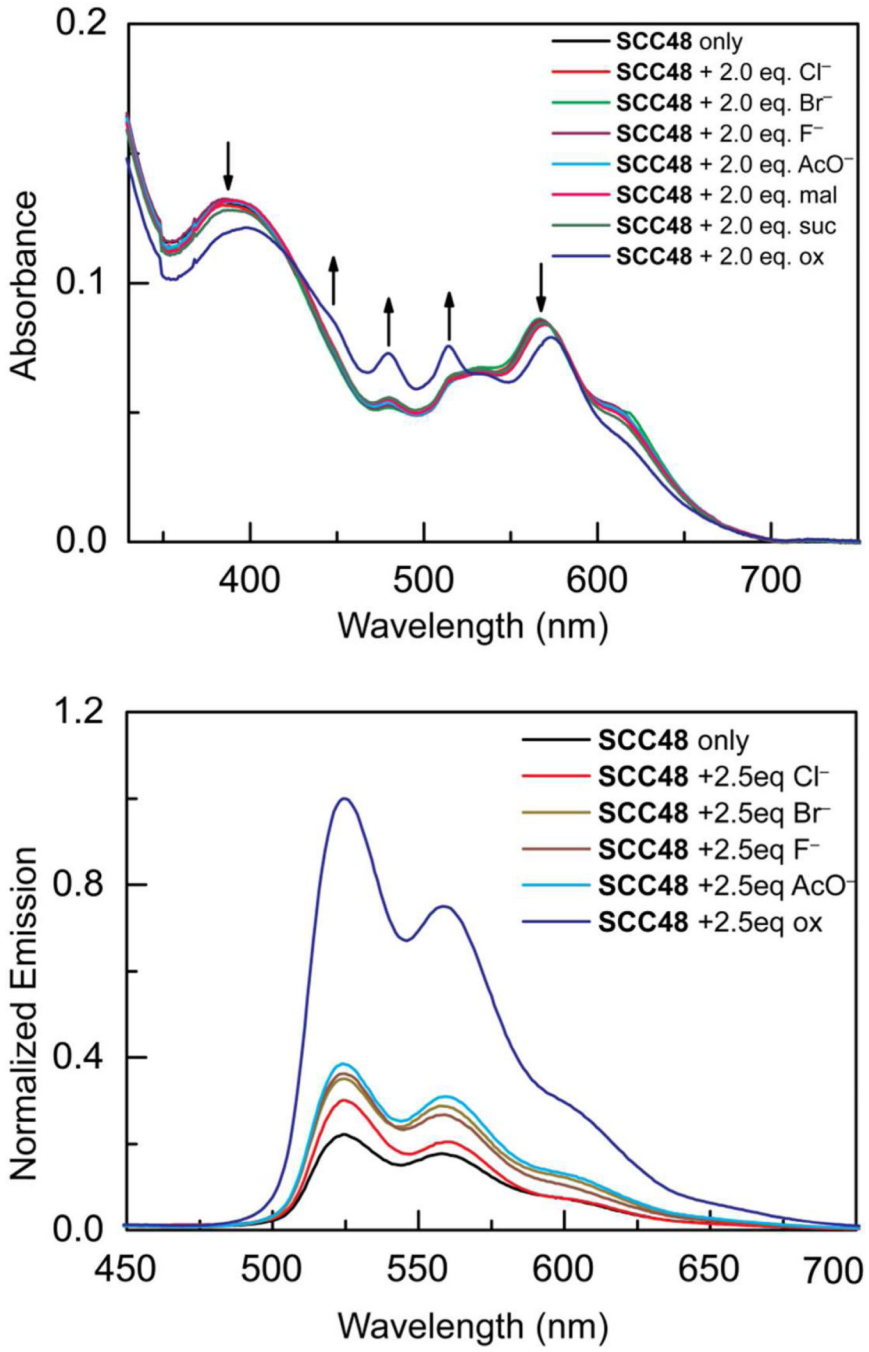

Figure 9.
Absorption and emission responses of **SCC48** to anionic analytes.

NIH-PA Author Manuscript

NIH-PA Author Manuscript

NIH-PA Author Manuscript

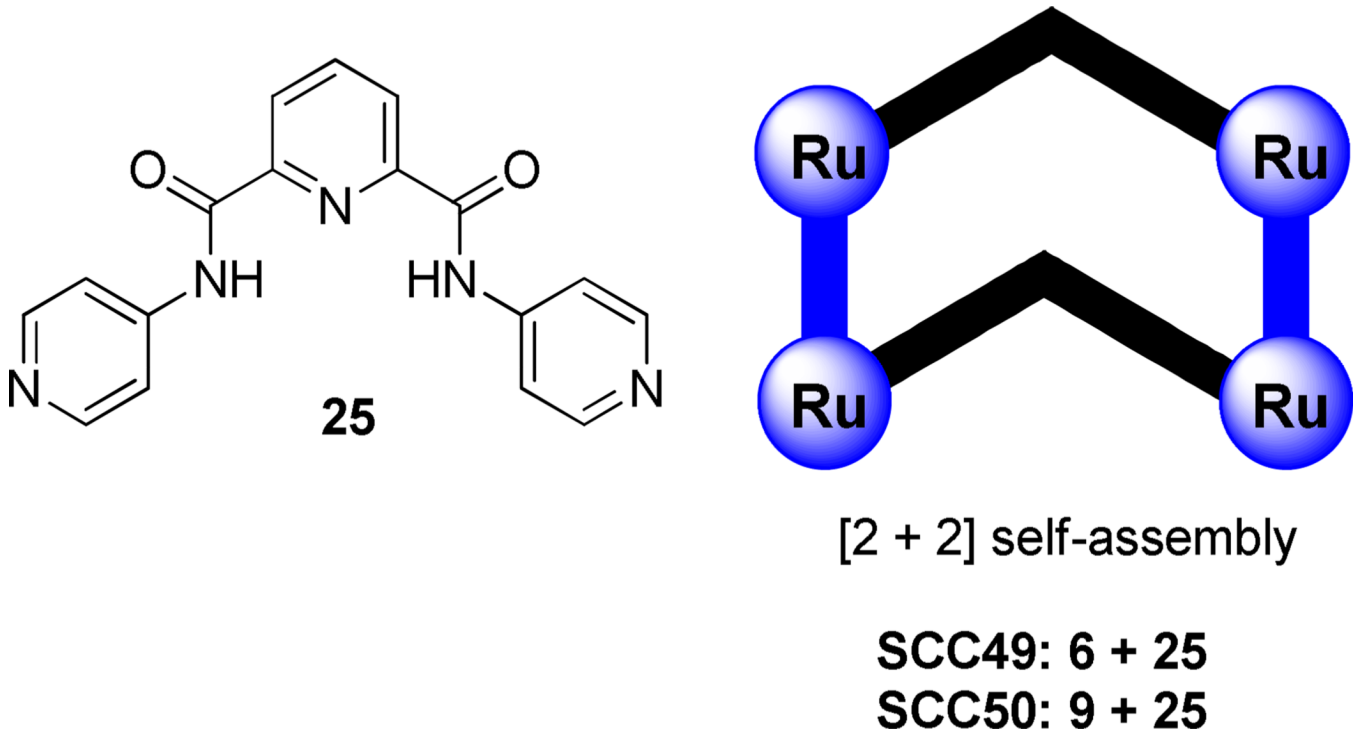

Figure 10.
Non-linear ditopic donors form wedge-shaped metallabowls when combined with molecular clips.

NIH-PA Author Manuscript
NIH-PA Author Manuscript
NIH-PA Author Manuscript

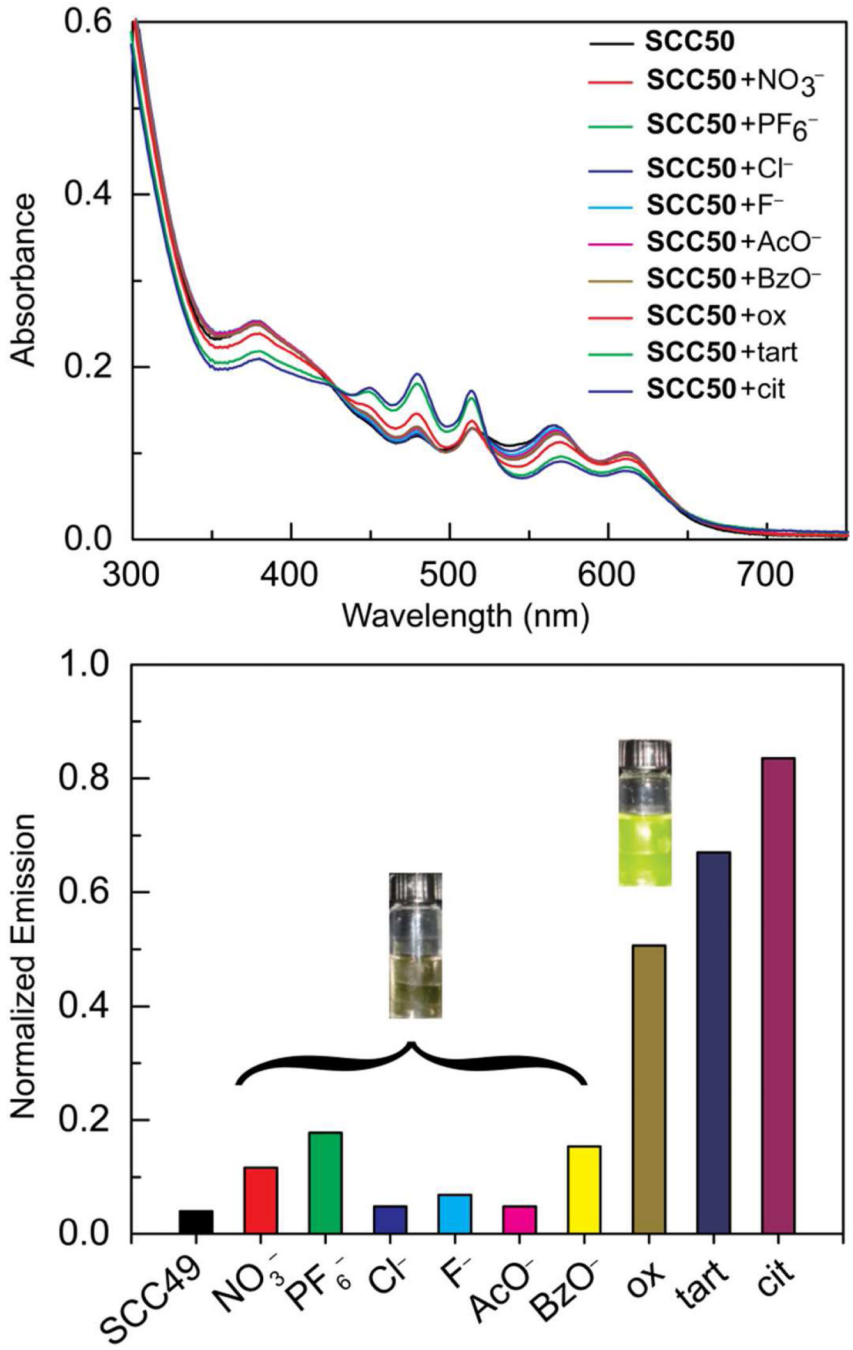

Figure 11.
Spectral responses of **SCC50** to the addition of anionic analytes.

NIH-PA Author Manuscript

NIH-PA Author Manuscript

NIH-PA Author Manuscript

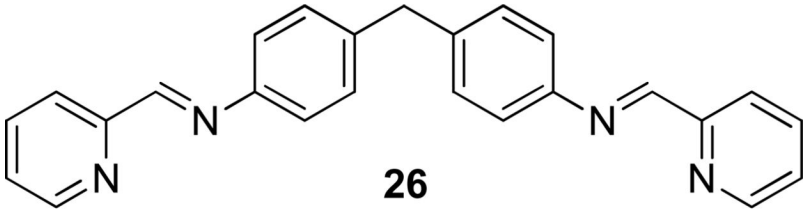

26

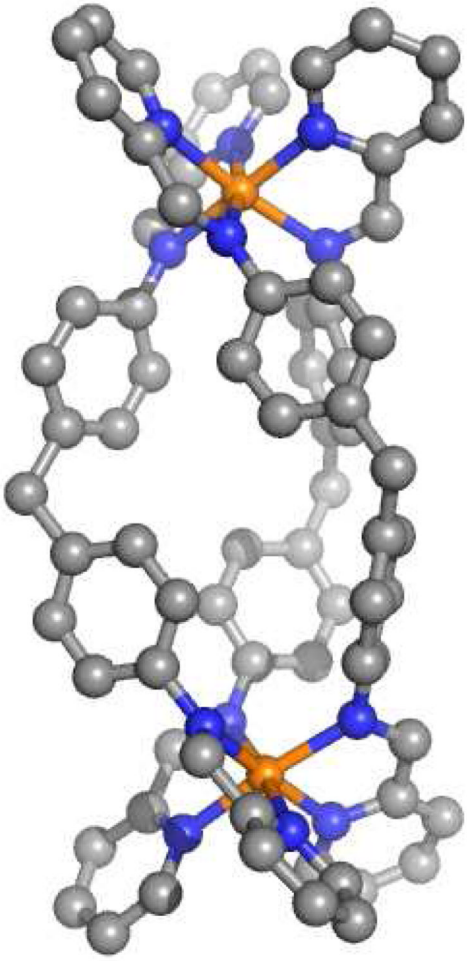

$[Ru_2(\mathbf{26})_3](PF_6)_4$: **SCC51**

Figure 12.
Structure M_2L_3 helicate **SCC51**. Solvent molecules, counterions and hydrogen atoms omitted.

NIH-PA Author Manuscript

NIH-PA Author Manuscript

NIH-PA Author Manuscript

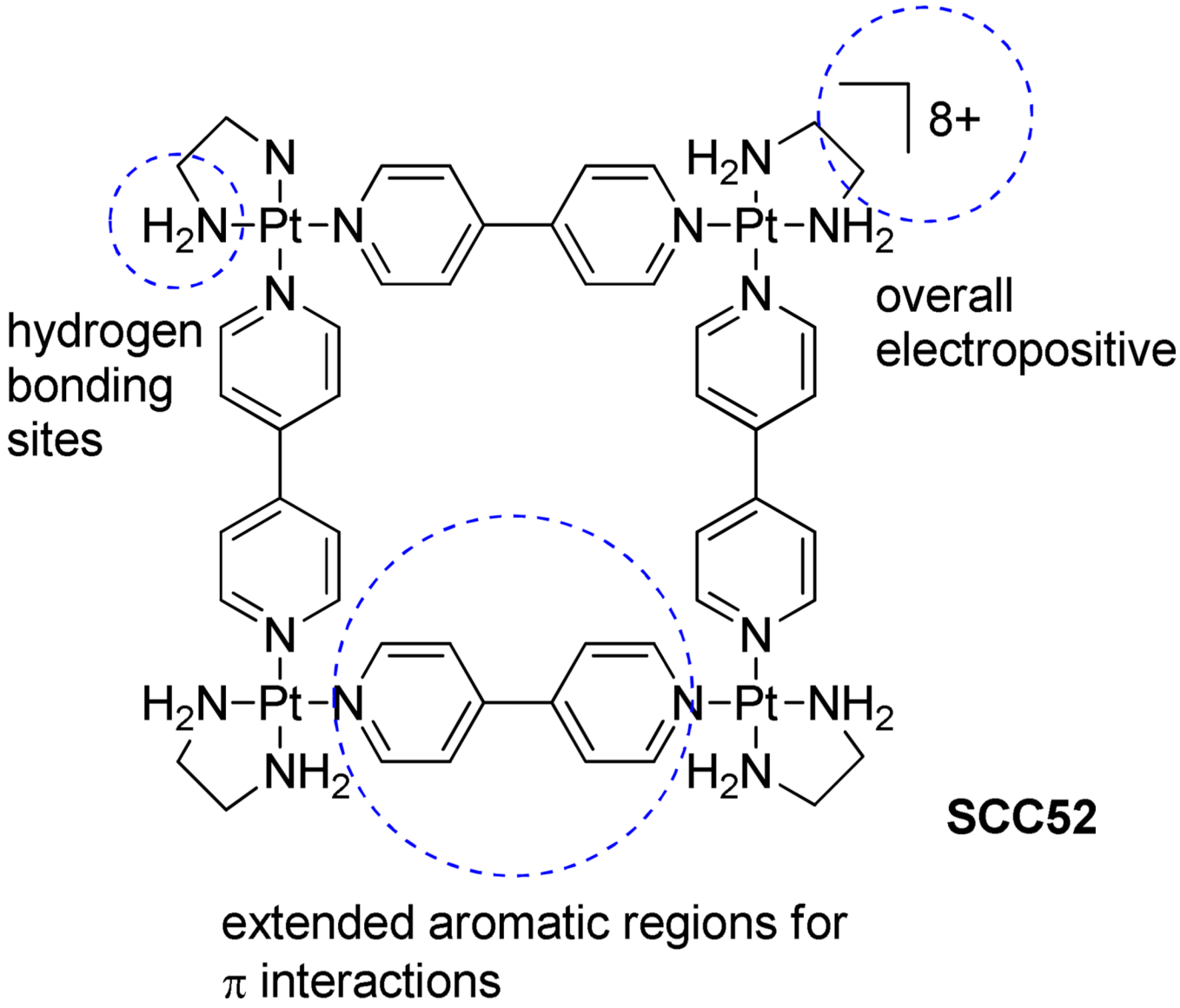

Figure 13.
Supramolecular squares possess many attractive features for G-quadruplex stabilization.

NIH-PA Author Manuscript

NIH-PA Author Manuscript

NIH-PA Author Manuscript

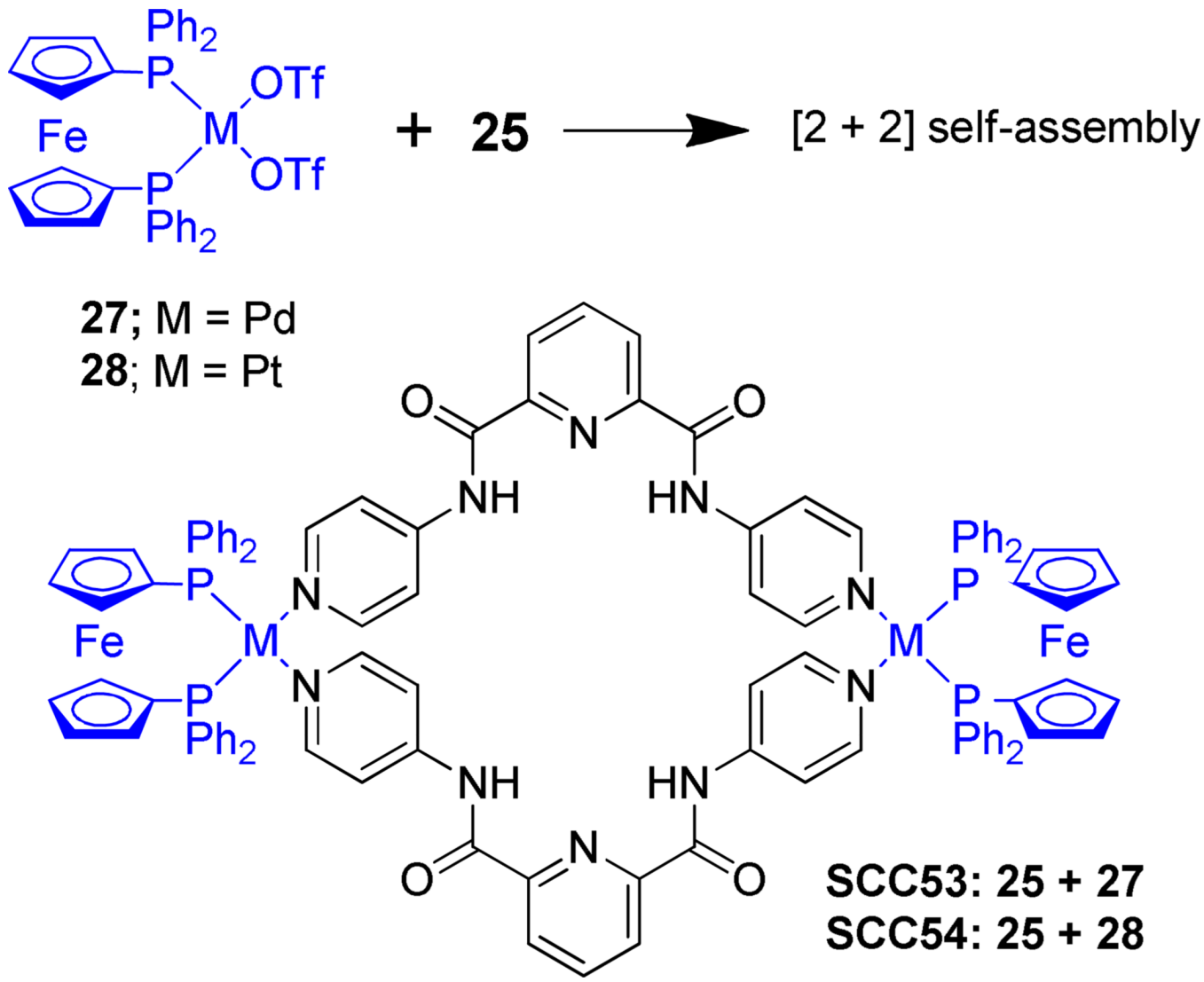

Figure 14.
Heterobimetallic SCCs formed via the assembly of non-linear ditopic donors with square planar metal precursors

NIH-PA Author Manuscript
NIH-PA Author Manuscript
NIH-PA Author Manuscript

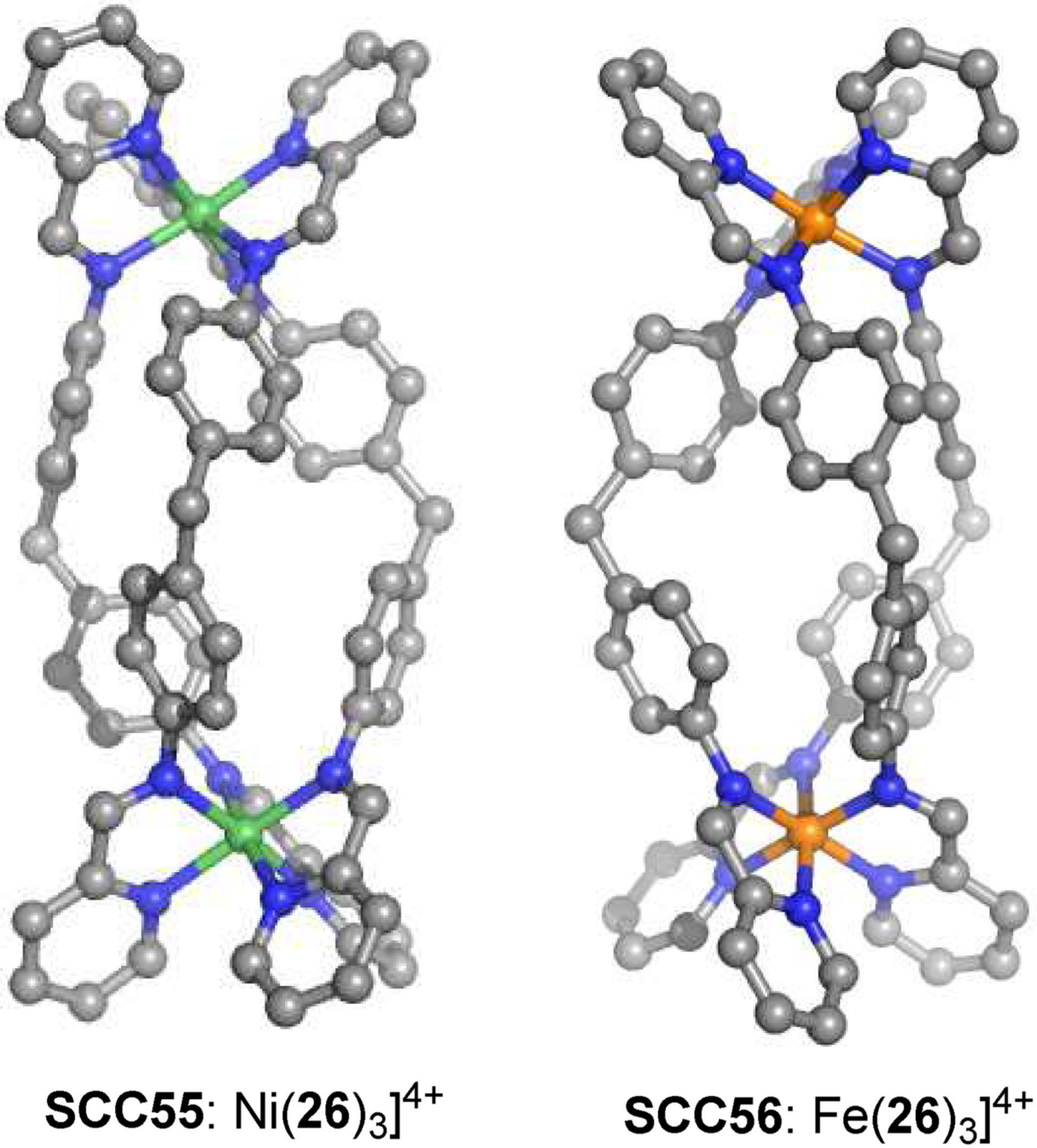

Figure 15.
X-ray crystal structures of Ni (*left*) and Fe (*right*) SCCs. Hydrogen atoms, solvents and counterions omitted for clarity.

NIH-PA Author Manuscript
NIH-PA Author Manuscript
NIH-PA Author Manuscript

Table 1

Cytotoxicities of Ru-based trigonal prisms

	Cell Line IC_{50} values				
	SK-hep-1	**HeLa**	**HCT-15**	**A-549**	**MDA-MB-231**
SCC2	83.7	163.7	187.9	inact	inact
SCC4	3.8	9.2	4.1	3.4	7.6
cisplatin	6.3	10.5	5.6	2.4	2.7

NIH-PA Author Manuscript

NIH-PA Author Manuscript

NIH-PA Author Manuscript

Table 2

Cytotoxicities of selected active rectangular SCCs.

	Cell Line IC_{50} values / μM (±)			
	SK-hep-1	**HeLa**	**HCT-15**	**AGS**
SCC6	5.36 (0.38)	9.40 (0.51)	9.83 (0.33)	2.65 (0.02)
SCC7	8.60 (0.65)	9.55 (0.87)	13.27 (0.03)	10.83 (0.30)
SCC8	51.08 (0.95)	14.91 (0.59)	11.40 (0.15)	9.61 (0.55)
SCC9	58.88 (0.08)	43.71 (2.08)	11.91 (0.10)	10.37 (0.69)
SCC10	15.45 (0.95)	20.48 (2.70)	15.23 (0.87)	11.65 (0.16)
SCC13	19.00 (4.99)	-	31.74 (5.49)	-
SCC16	114.05 (2.69)	-	109.60	31.96 (2.25)
SCC19	6.97 (0.69)	-	7.46 (0.24)	-
SCC20	29.53 (1.72)	-	39.45 (1.73)	-
SCC21	66.19 (0.25)	-	53.66 (0.27)	-
SCC22	63.58 (1.27)	-	57.05 (0.98)	-
SCC23	9.60 (0.84)	-	10.66 (0.19)	-
SCC24	16.32 (1.98)	-	17.68 (0.92)	-
6	>200	-	-	-
7	>200	-	-	-
8	149.00 (2.01)	-	-	-
9	>200	-	-	-
cisplatin	12.38 (0.24)	76.85 (0.41)	8.38 (2.31)	> 100
dox	2.67 (0.24)	3.16 (0.04)	15.34 (0.58)	0.70 (0.16)

dox = doxorubicin

NIH-PA Author Manuscript

NIH-PA Author Manuscript

NIH-PA Author Manuscript

Table 3

Cytotoxicities of Ru-based molecular clips and isomer mixtures of SCCs containing asymmetric donors.

	Cell Line IC_{50} values / μM			
	A-549	**Colo320**	**H1299**	**MCF7**
1 (oxalato)	40.94	51.01	>100	>100
2 (donq)	18.05	12.95	>100	63.97
SCC44	38.86	>100	>100	80.91
SCC45	10.18	0.33	3.62	< 0.1
Cisplatin	>100	38.6	>100	>100

NIH-PA Author Manuscript

NIH-PA Author Manuscript

NIH-PA Author Manuscript

Table 4

Cytotoxicities of bis-benzimidazole-based SCCs

	Cell Line IC_{50} values / μM			
	A-549	**Colo320**	**H1299**	**MCF7**
24	>100	>100	>100	>100
SCC46	78.86	15.42	15.65	8.41
SCC47	13.94	>100	>100	80.91
Cisplatin	38.6	>100	>100	>100